

Scintillator Materials—Achievements, Opportunities, and Puzzles

M. Nikl, E. Mihokova, J. Pejchal, A. Vedda, M. Fasoli, I. Fontana, V. V. Laguta, V. Babin, K. Nejezchleb, A. Yoshikawa, H. Ogino, and G. Ren

Abstract—Participation of shallow and deep traps in the processes of energy transfer and capture is studied by means of time-resolved emission spectroscopy and thermoluminescence in several groups of the Ce^{3+} and Pr^{3+} -doped complex oxide single crystal scintillators. Tunnelling-driven recombination processes are distinguished in all the groups of examined materials: closely spaced electron and hole traps give rise to the t^{-1} phosphorescence decays at low temperatures in the Ce-doped aluminum garnets and perovskites, while thermally assisted tunneling process is proposed to explain temperature independent trap depth in glow curve peaks within 50–250°C in Ce-doped lutetium orthosilicates.

Index Terms—LuAG:Ce, LuAG:Pr, LuYAP:Ce and LYSO:Ce single crystals, points defects and traps, scintillators.

I. INTRODUCTION

DESPITE the relatively long history of the development of scintillator and phosphor materials started at the end of 19th century, within the last two decades the scintillator characteristics and figure-of-merit of a number of new materials were studied and some of the materials were successfully industrialized. In particular, Ce-doped silicates, aluminum perovskites

Manuscript received June 28, 2007; revised September 27, 2007. This work was supported by the Czech GACR 202/05/2471, MSM KONTAKT ME903, ME953, GA AV S100100506 and "Italian Cariplo foundation 2006-2008 structure and optical properties of self-organized nano- and mesoscopic materials" projects and by the EC—Research Infrastructure Action under the FP6 "Structuring the European Research Area" Program (through the Integrated Infrastructure Initiative Integrating Activity on Synchrotron and Free Electron Laser Science).

M. Nikl is with the Institute of Physics AS CR, 162 53 Prague, Czech Republic and also with the Department of Materials Science, University of Milano-Bicocca, 20125 Milan, Italy (e-mail: nikl@fzu.cz).

E. Mihokova and J. Pejchal are with the Institute of Physics AS CR, 162 53 Prague, Czech Republic (e-mail: mihokova@fzu.cz; pejchal@fzu.cz).

A. Vedda, M. Fasoli and I. Fontana are with the Department of Materials Science, University of Milano-Bicocca, 20125 Milan, Italy (e-mail: anna.vedda@mater.unimib.it; mauro.fasoli@mater.unimib.it; ilaria.fontana@mater.unimib.it).

V. V. Laguta is with the Institute of Problems in Materials Science UAS, 03142 Kiev, Ukraine and also with the Institute of Physics AS CR, 162 53 Prague, Czech Republic (e-mail: laguta@ipms.kiev.ua).

V. Babin is with the Institute of Physics, University of Tartu, 51 014 Tartu, Estonia (e-mail: vladimir.babin@ut.ee).

K. Nejezchleb is with the Crytur Ltd., 51119 Turnov, Czech Republic (e-mail: nejezchleb@crytur.cz).

A. Yoshikawa is with IMRAM, Tohoku University, 980-8577 Sendai, Japan (e-mail: yosikawa@tagen.tohoku.ac.jp).

H. Ogino is with the School of Engineering, The University of Tokyo, 113-8656 Tokyo, Japan (e-mail: tuogino@mail.ecc.u-tokyo.ac.jp).

G. Ren is with the Shanghai Institute of Ceramics (SIC), 200050 Shanghai, China (e-mail: rgh@mail.sic.ac.cn).

Color versions of one or more of the figures in this paper are available online at <http://ieeexplore.ieee.org>.

Digital Object Identifier 10.1109/TNS.2007.913480

and garnets, trivalent-ion-doped $PbWO_4$ and Ce-doped binary rare earth halides are worth mentioning, for recent reviews see [1]–[4]. An interest in new scintillator materials is pushed by increasing number of medical, industrial or scientific applications, requiring higher material performance. To optimize materials towards their intrinsic limits, understanding of energy transfer and storage processes, specific defects and their relation to the manufacturing technology appear of crucial importance [1], [4]. Deep electron traps and their role in the afterglow of the Ce-doped silicates, shallow electron traps related to antisite defects in aluminum garnets or appearance of slower scintillation components and drop of the light yield in mixed (Y-Lu) aluminum perovskites are just a few examples of current problems in the field. These problems should be studied and appropriate technological solutions should be found to further improve the material performance.

The aim of this paper is to review the current understanding of the role of selected defects in the processes of energy transfer and carrier capture in the above mentioned materials belonging to complex oxide scintillators.

II. SAMPLES AND EXPERIMENTAL TECHNIQUE

Ce-doped single crystals of $Lu_3Al_5O_{12}$, (Y-Lu) AlO_3 and Lu_2SiO_5 were grown in some of the institutions where the coauthors belong, namely: CRYTUR (perovskites $YAlO_3$ (YAP), (Lu-Y) AlO_3 (LuYAP) and garnets $Lu_3Al_5O_{12}$ (LuAG)) or SIC (silicates Lu_2SiO_5 (LSO), Y_2SiO_5 (YSO), (Lu-Y) $_2SiO_5$ (LYSO)) by Czochralski method from the high temperature melt from the raw materials with at least 4N purity. Pr-doped and Ga-admixed aluminum garnets were grown in IMRAM from the raw materials of the same purity using the micropulling-down (m-PD) and Czochralski methods. Plates up to $7 \times 7 \times 1$ mm, polished to an optical grade, were prepared for luminescence experiments.

Measurements of photoluminescence (PL) and radioluminescence (RL) spectra as well as the PL and scintillation decays, were performed with the Spectrofluorometer 199S (Edinburgh Instruments) equipped with pulsed UV flashlamps, steady-state H₂-lamp and X-ray tube (35–40 kV, Mo-anticathode) and ^{22}Na radioisotope (511 keV photons) excitation sources. Emission spectra were corrected for the spectral response of the system. Convolution of the multi-exponential function with the instrumental response was used to find the correct decay-time values in the decays extended to ns time scales. TSL measurements were performed after X-irradiation at 10 K (by a Philips 2274 X-ray tube operated at 20 kV) or at RT (by a Machlett OEG50 X-ray tube operated at 30 kV). In the low-T range (10–300 K)

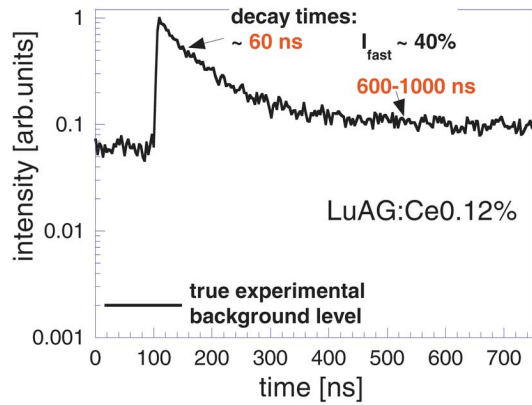


Fig. 1. Spectrally unresolved scintillation decay of the 0.12%Ce-doped sample excited at RT by 511 keV photons from ^{22}Na radioisotope.

we performed wavelength resolved measurements with a detection system using a monochromator coupled to a CCD detector (Jobin-Yvon Spectrum One 3000) operating in the 280–710 nm interval. A heating rate of 0.1 K/s was adopted. High-T measurements (from RT to 400°C) were performed with a heating rate of 1°C/s and TSL emission was detected by a photomultiplier (EMI9635QB).

III. EXPERIMENTAL RESULTS AND DISCUSSION

A. Ce- and Pr-doped Aluminum Garnets

Ce^{3+} -doped $\text{Y}_3\text{Al}_5\text{O}_{12}$ (YAG) single crystal for fast scintillator applications was reported in the literature already in the seventies [5]. The first comprehensive description of YAG:Ce scintillator characteristics was reported by Moszynski *et al.* [6], who included this material in the high figure-of-merit oxide scintillators. Isostructural LuAG has a higher density (6.67 g/cm³) than YAG (4.56 g/cm³), which is advantageous in the case of hard X- and γ -ray detection. LuAG:Ce scintillator became of interest relatively recently [7], [8]. The m-PD grown Pr-doped LuAG scintillator was for the first time mentioned in the literature in 2005 [9] and further improved using the Czochralski technique [10]: light yield approaching 300% of $\text{Bi}_4\text{Ge}_3\text{O}_{12}$ (BGO), spectrally uncorrected, and the dominant decay time of about 20 ns include this material in the group of the fastest, high light yield and high density materials available today.

Recent studies revealed a considerable percentage of slow, technically unexploitable light in the scintillation response of aluminum garnet scintillators, especially in those LuAG-based [11]. Typical scintillation decay of LuAG:Ce is given in Fig. 1. While the dominant component has a decay time very similar to that of PL decay (54 ns), a slower decay process that can be fit by an exponential with 600–1000 ns decay time is always found.

Moreover, the signal increase before the rising edge of the decay (with respect to the true experimental background level given essentially by the detector electronic noise) points to the presence of very slow decay processes the time constant of which is comparable with the time interval between two subsequent excitation events (tens-to-hundreds of microseconds)

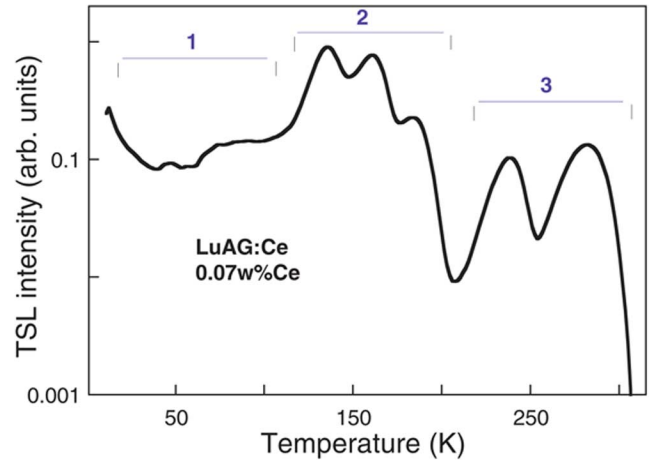


Fig. 2. TSL glow curve of LuAG:Ce after X-irradiation at 10 K.

[11]. The low temperature TSL glow curve reveals a number of trapping states and three typical regions can be distinguished (so far more than twenty different single crystals of Ce^{3+} and Pr^{3+} doped LuAG have been measured), see Fig. 2. Region 2 is related to the shallow electron trap due to an antisite Lu_{Al} defect (AD) [12], [13], responsible also for the intrinsic luminescence of undoped LuAG, see Fig. 3. ADs in isostructural YAG were already evidenced by Ashurov *et al.* a time ago [14]. Recent theoretical calculations show that creation of these defects in aluminum garnets is relatively easy [15]. The trap depth related to two dominant peaks at about 140 K and 165 K in LuAG:Ce was calculated to be about 0.31 eV and 0.38 eV, respectively. The dose dependence of the TSL glow curve confirmed the first order recombination process. Therefore detrapping times for both traps at RT could have been calculated and the values of about 50 μs and 450 μs , respectively, were obtained. Apparently, thermally induced detrapping from these traps into the conduction band followed by delayed radiative recombination at Ce^{3+} ions cannot explain the slower, sub-microsecond component in the scintillation decay (Fig. 1). As spatially-correlated AD- Ce_{Lu} pairs were found with the help of EPR and tunneling recombination between related electron and hole trapped at such pairs was suggested at least within 10–40 K (region 1 in Fig. 2) [16], it seems reasonable to consider tunneling recombination process to explain also slower, sub-microsecond decay component in the RT scintillation decay.

In the search for further optimization of LuAG-based scintillator a systematic attention was paid to reduce the trapping effects related to the Lu_{Al} AD electron trap. We found that Ga-admixed LuAG with the formula $\text{Lu}_3(\text{Ga}_{0.4}\text{Al}_{0.6})_5\text{O}_{12}:\text{Pr}$ shows considerably lower TSL intensity and rather structureless TSL pattern shifted to lower temperatures with respect to LuAG:Pr [12]. Furthermore, its scintillation decay was significantly accelerated. Another set of samples with Ga relative content 0.05, 0.1 and 0.2 was prepared to study Ga-concentration dependence of trapping phenomena in Pr-doped Lu(Ga,Al)G host. While the host luminescence due to the AD defect was efficiently suppressed already at the lowest Ga concentration [17], TSL glow curve shows smooth shift to lower temperatures and lower intensities, Fig. 4. VUV excitation spectra measured for some of

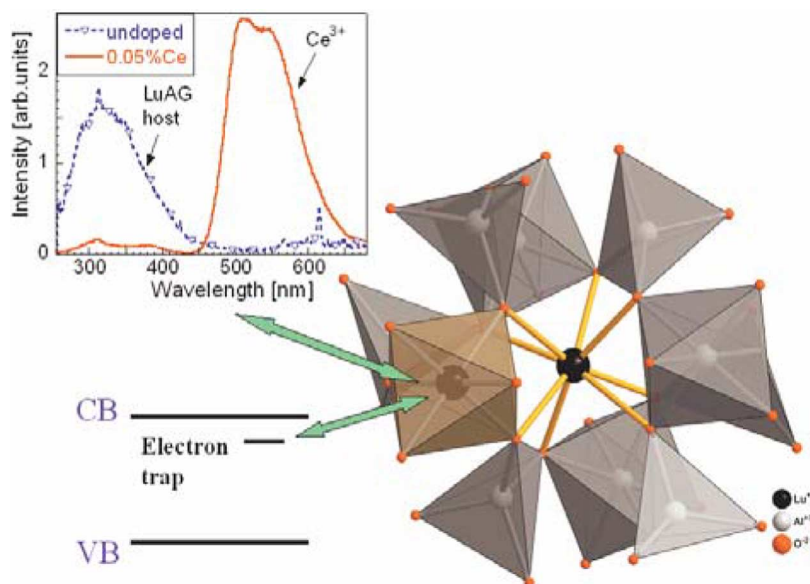


Fig. 3. The Lu_{Al} antisite defect in the LuAG structure. Resulting electron trap in the material forbidden gap is sketched on the left. Emission band within 300–350 nm due to antisite defect and its competition with that of the Ce^{3+} center can be derived from radioluminescence spectra at RT—upper left. Emission lines around 312 nm and 615 nm in the undoped sample are due to Gd^{3+} and Eu^{3+} accidental impurities, respectively.

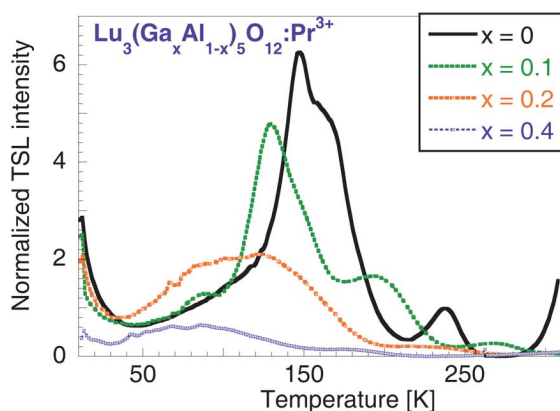


Fig. 4. TSL glow curves after x-irradiation at 10 K for Ga-admixed LuAG.

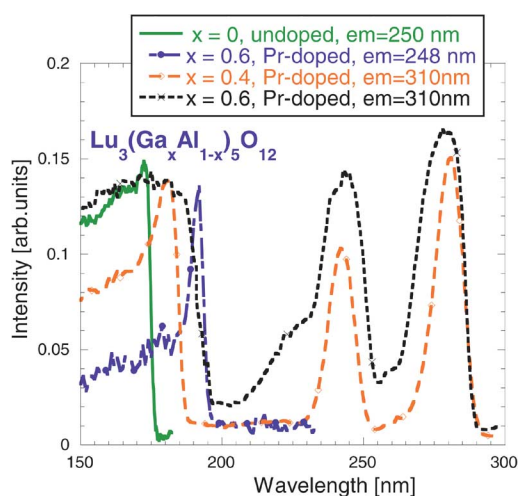


Fig. 5. Excitation spectra of undoped and Pr-doped $\text{Lu}_3(\text{Ga}_x\text{Al}_{1-x})_5\text{O}_{12}$ single crystals at 10 K.

these samples show a host band-edge shift towards lower energies. For the $\text{Ga}_{0.4}$ concentration it is of about 0.4 eV, which is comparable with the Lu_{Al} trap depth mentioned before, Fig. 5. TSL gradual change in Fig. 4 does not point to a 1:1 suppression of the Lu_{Al} defects due to the Ga admixture. Given the value of the band edge shift it rather seems that the levels of Lu_{Al} defects become gradually buried in the lowered bottom of the conduction band, which becomes dominated by the Ga wave functions.

Additional shift of the band edge towards lower energies for Ga admixture greater than 0.4 can be related to increasing occupancy of tetrahedral Al sites by Ga. Their energy levels are expected to be lower with respect to the garnet octahedral sites [18]. Despite the gradual acceleration of scintillation decay with increasing Ga content the light yield does not increase with respect to the Ga-free LuAG:Pr and overall radioluminescence intensity gets even lower, Fig. 6. This may indicate that Ga admixture induces additional nonradiative losses. Further systematic studies are needed to explain the observed characteristics.

B. Ce-Doped Aluminum Perovskites

Luminescence of $\text{YAlO}_3:\text{Ce}$ (YAP:Ce) was reported by Weber [19], while the favourable properties of this material for scintillation applications were described later by Takeda *et al.* [20] and Atrata [21]. $\text{LuAlO}_3:\text{Ce}$ became of interest in the mid nineties due to its higher density and effective atomic number [7], [22], [23] and later on also the mixed $\text{Lu}_x\text{Y}_{1-x}\text{AlO}_3:\text{Ce}$ crystals were prepared and characterized [24], [25]. A review paper devoted to this group of scintillation materials has been published recently [1].

The 370 nm emission of Ce^{3+} center in YAP shows a single-exponential fast PL decay with the decay time of about 17 ns. Somewhat longer scintillation decay time between 22 and 38 ns followed by a minor slower component with a decay time

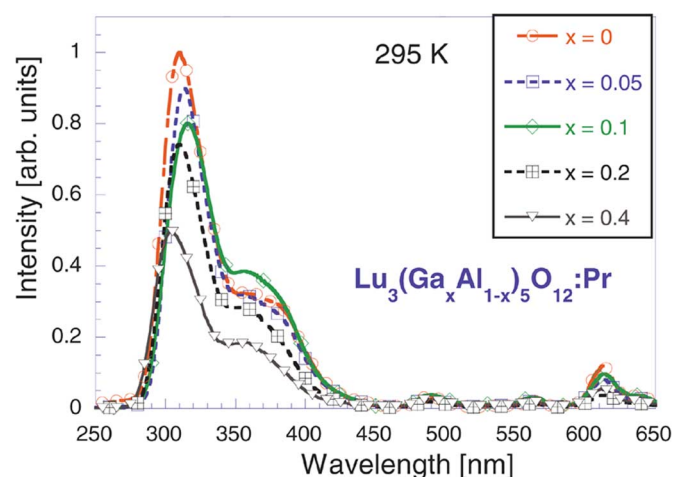


Fig. 6. Radioluminescence spectra at RT. Excitation by an X-ray tube, 40 kV.

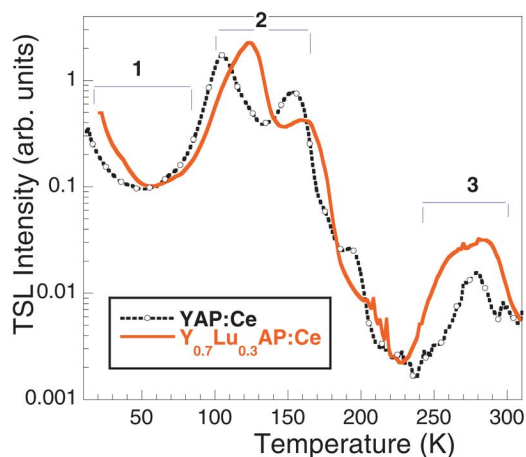


Fig. 8. TSL glow curves after irradiation at 10 K of YAP:Ce and LuYAP:Ce.

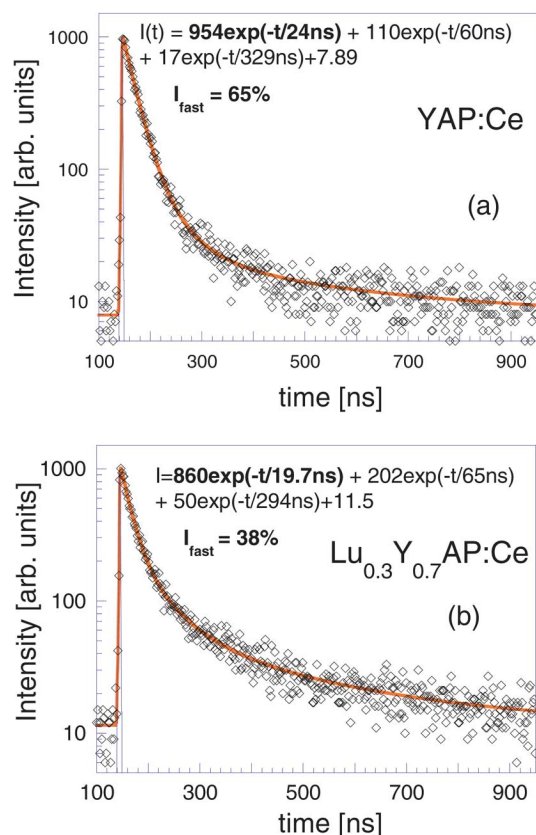


Fig. 7. Spectrally unresolved scintillation decays of LuAP:Ce (a) and LuYAP:Ce (b) excited by 511 keV of ^{22}Na radioisotope at RT.

of a few hundreds of nanoseconds is evaluated in the scintillation decay [26], [27]. The latter component can be explained by delayed recombination of charge carriers at Ce^{3+} centres (similarly as in aluminum garnets). The scintillation response of pure LuAP:Ce is dominated $\sim 80\%$ of the overall intensity) by a fast decay component of about 17–19 ns, while the rest of the intensity is released with a decay time of 160–180 ns.

In the case of Lu-rich mixed ($x = 0.65 - 0.7$) crystals, the intensity of the fast component is considerably reduced (40–54%) and, accordingly, the second slower component

with the decay time of about 190 ns becomes more intense [28]. A comparison of scintillation decays of YAP:Ce and $\text{Lu}_{0.3}\text{Y}_{0.7}\text{AlO}_3:\text{Ce}$ is given in Fig. 7(a) and (b). Apparently, there is an increase of the slower scintillation process and similar situation as in the Lu-rich $\text{Lu}_x\text{Y}_{1-x}\text{AlO}_3:\text{Ce}$ occurs. Thus, while the limit YAP:Ce and LuAP:Ce compositions show dominating fast emission component with the decay time of about 20 ns, the relative content of slower processes in the mixed compounds considerably increases. Fig. 8 displays the TSL glow curves of the above mentioned two samples after X-irradiation at 10 K. One can distinguish three typical regions in YAP:Ce (more than ten different YAP:Ce single crystals have been studied for TSL characteristics so far). Regions 1 and 2 resemble those found in YAG:Ce and within the region 1 the YAP:Ce phosphorescence decay exactly follows the t^{-1} form as shown in detail in [29]. It is interesting to note that based on comparison with the optical ceramics the 92 K glow curve peak in YAG:Ce was interpreted as due to the AD-related electron trap [30]. In the undoped and Ce-doped YAP the glow curve peak at around 150 K has been ascribed to the thermal decay of an O^- center [16]. The dose dependence of glow curves confirmed the first order TSL recombination kinetics of both 105 K and 150 K peaks. Therefore corresponding detrapping times at RT were easily calculated, yielding the values of about 100–200 μs [29]. Consequently, retrapping of migrating carriers at RT due to the traps related to the 105 K and 150 K glow-curve-peaks induces similar delays with respect to LuAG:Ce described earlier. However, one has to point out that relative intensity of TSL peaks in region 3 is much higher in LuAG:Ce, (see Fig. 2), than in YAP:Ce (Fig. 8). Much longer corresponding detrapping times at RT are expected, i.e., related traps in region 3 would have more detrimental effect on the time characteristics and light yield (LY) of such a scintillator.

Admixture of Lu into YAP:Ce results in the shift of the position of the dominant TSL peak up to about 125 K and to peak broadening, Fig. 8. Furthermore, relative intensity of TSL peaks in region 3 is enhanced. Whatever is the nature of related electron traps, the admixture of Lu into YAP:Ce is thus expected to slow down retrapping processes due to these traps, which may show a detrimental influence on the value of LY.

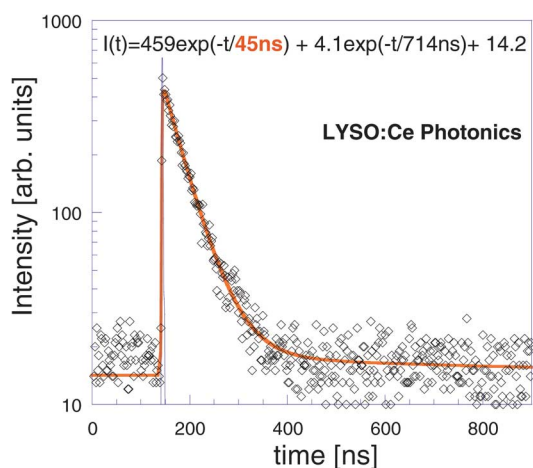


Fig. 9. Spectrally unresolved scintillation decay at RT. Solid line is the convolution of instrumental response (also in the figure) with the function $I(t)$ given in the figure.

C. Ce-Doped Orthosilicates

Scintillation characteristics of Ce-doped rare-earth (RE) oxyorthosilicates were for $Gd_2SiO_5:Ce$ (GSO) reported more than 20 years ago [31]. Optical studies of Ce-doped samples showed two Ce^{3+} emission bands related to two different Ce^{3+} crystallographic sites in GSO, LSO, and YSO [32]. In LSO:Ce the doublet emission peaking at 393 nm and 427 nm was ascribed to “ Ce_1 ” center, the luminescence of which is not quenched up to RT. On the other hand, the composite emission peaking at 460 nm, well detected only below 80 K, was ascribed to the “ Ce_2 ” center. The presence of two distinct Ce^{3+} emissions is in accordance with the existence of two Lu^{3+} crystallographic sites and with the incorporation of Ce as a substitute for Lu. ESR measurements support this assumption since Ce^{3+} ions are found at both lutetium sites. As the ESR intensity is directly linked to the concentration of paramagnetic ions, the relative Ce^{3+} concentration in each site could have been determined. The values are: $Ce_1 = 95\%$ and $Ce_2 = 5\%$. The most substituted site is attributed to the larger Lu_1 site with 6 + 1 oxygen neighbors [33].

In contrast to aluminum perovskites and garnets the scintillation decay of Ce-doped LSO or LYSO shows the only component with the decay time somewhat longer with respect to the PL one (35 ns), Fig. 9. Moreover, there is practically no difference between the decays of Ce-doped LSO and LYSO (with a typical 5–10% of Y admixing).

TSL glow curve of LYSO:Ce with a relatively high LY (Photonics Material, see ref. 34 for LY measurements) is displayed in Fig. 10 together with those of LuAG:Ce and YAP:Ce. Concentration of Ce^{3+} in these YAP, LYSO and LuAG samples is determined from the optical absorption spectra and using an ICP chemical analysis of about 8000 ppm, 1300 ppm and 2400 ppm, respectively. One can immediately see that the amplitude of TSL signal in LYSO:Ce is 1–2 orders of magnitude lower with respect to that of the other two samples indicating the lack of shallow electron traps in silicates with respect to aluminum perovskite and garnet hosts. This is consistent with the absence of slower decay components in LYSO:Ce scintillation response (Fig. 10).

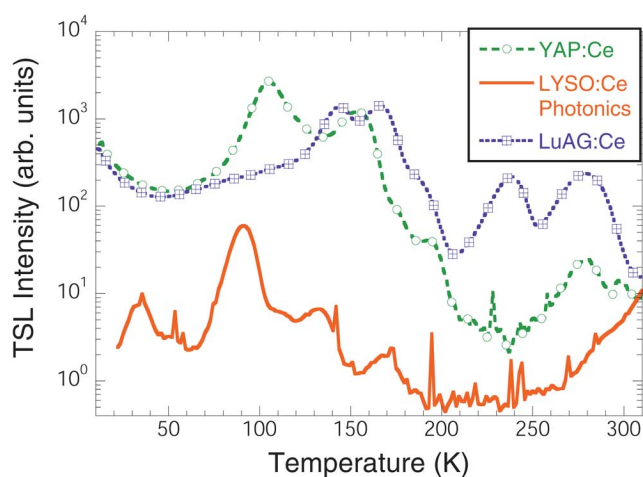


Fig. 10. TSL glow curves of YAP:Ce, LuAG:Ce and LYSO:Ce after X-irradiation at 10 K. Curves can be compared quantitatively.

Another advantage of LSO host consists in low thermal stability of intrinsic emission centres based on self-trapped excitons or holes, which persist only up to about 50 K, and then are thermally disintegrated [35]. Thus host-related slower emissions do not delay an energy transfer towards Ce^{3+} in any noticeable manner, while emission related to the presence of AD in YAG/LuAG host survives up to RT and is in competition with that of Ce^{3+} under high energy excitation [36].

In the case of LSO, it was soon recognized that it presents a fairly strong afterglow at RT [37]. Fundamental studies focusing on the comprehension of the microscopic physical mechanism governing afterglow were carried out in order to find possible technological solutions. The activation energy of the process was found to be approximately 1 eV [37]; it is in accordance with the calculated trap depth of the leading TSL peak situated at 375 K and 340 K (using a heating rate of 6 K/s and 0.24 K/s, respectively). Hence, mentioned afterglow appears to be due to RT carrier detrapping from the trap responsible for this TSL peak followed by radiative recombination at Ce^{3+} luminescent centers. Actually the 340 K peak (heating rate 0.24 K/s) is the first one of a series of as many as 6 peaks observed in the glow curve above RT, Fig. 11. Its spectral emission coincides with the $Ce^{3+} 5d-4f$ transition [37]. Annealing experiments in reducing or oxidizing atmosphere led to the suggestion that traps could be related to oxygen vacancies [38]. Indeed, TSL glow curves above RT show a very similar pattern for both LSO and LYSO samples coming from different manufacturers, Fig. 11. Evaluation of the trap depth for all of the glow peaks in LYSO:Ce (G.Ren) sample in Fig. 11 was made using the partial cleaning method, see e.g., [39], [40] for details, and the obtained values are reported in Fig. 12. Interestingly, with the exception of the 305°C peak of the trap depth of about 1.5 eV, the trap depth within 30–260°C is very little temperature dependent in contrast to usual situation, in which a step-like dependence of the trap-depth on increasing temperature is obtained (for LuAG:Ce see [40]). A very similar situation was found in YAP:Ce and LuYAP:Ce [39] and was explained as due to a thermally assisted tunnelling of electrons trapped at oxygen vacancies towards holes trapped at Ce ions at discrete distances (given by

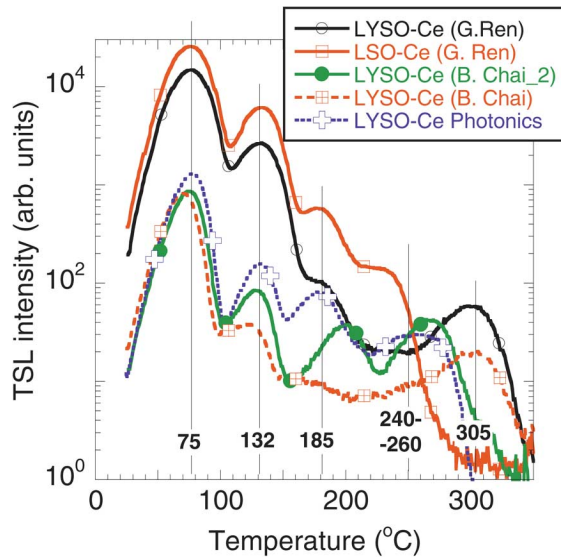


Fig. 11. TSL glow curves after X-irradiation at RT at LSO:Ce and LYSO:Ce.

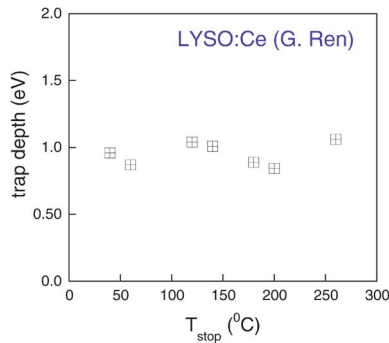


Fig. 12. Temperature dependence of the trap depth on T_{stop} in the partial cleaning procedure, for details see [39].

the crystal structure), followed by their radiative recombination. The same consideration can be done in LSO(LYSO):Ce so that it is tentatively proposed that such thermally assisted tunneling between an oxygen vacancy-based electron trap and Ce_1 hole trap is responsible for the observed TSL glow curve pattern above RT up to some 260°C.

IV. CONCLUSIONS

Participation of various trapping states in the aluminum perovskites and garnets and in the orthosilicate scintillators was studied by correlated experiments using time-resolved luminescence spectroscopy and thermoluminescence.

Dominating shallow electron trap in aluminum garnets is ascribed to the Y_{Al} and Lu_{Al} antisite defects, which gives rise to the 92 K and triple 142–165–190 K TSL glow curve peaks, respectively. At RT the calculated detrapping times from related traps to conduction band for LuAG:Ce are longer than $\sim 50 \mu\text{s}$, so that this mechanism cannot be responsible for the existence of slower submicrosecond component in LuAG:Ce scintillation decay. Due to the evidence of tunneling-driven radiative recombination in the spatially correlated Ce^{3+} -AD pairs at low temperatures, this mechanism is proposed to explain the observed scintillation decay pattern at RT as well.

At RT the detrapping times related to the 105 K and 150 K TSL peaks in YAP:Ce are of the same order as those related to the antisite-defect related trap in LuAG:Ce and the absolute intensity of peaks is comparable as well. However, relative amplitude of the glow curve peaks within 200–300 K is noticeably higher in LuAG:Ce, which might be the reason for its lower LY.

Admixture of Lu into YAP host results in the high temperature shift and amplitude increase of the dominant 105 K peak. TSL intensity between 200–300 K is enhanced as well. All these phenomena can increase detrapping times at RT and effectively lower the light yield values. However, consistent TSL study over the full concentration range of the YAP-LuAP solid solution is necessary to understand in detail particular features of energy transfer and capture in the mixed systems.

Quantitative comparison of low temperature TSL glow curves among the Ce-doped aluminum perovskites, garnets and orthosilicates points to the lack of shallow electron traps in orthosilicates resulting in faster energy transfer from the host towards the Ce^{3+} ions. Another advantage of orthosilicate host is due to comparatively lower thermal stability of self-trapped exciton and hole states. These states become thermally disintegrated above 50 K and enable faster energy migration to the Ce^{3+} ions in comparison with aluminum garnets. These two factors are recognized as crucial in explanation of higher light yield values obtained at LSO:Ce and LYSO:Ce.

Temperature independence of trap depth corresponding to the TSL glow curve peaks within 40–260°C in LSO:Ce and LYSO:Ce cannot be explained by usual detrapping mechanism via conduction band. Instead, thermally assisted tunneling mechanism is proposed to explain the observed features similarly as earlier reported in the literature for YAP:Ce.

Obtained results point to possible space correlation and relative vicinity between the emission center (Ce^{3+} , Pr^{3+}) and an electron trap (antisite defect, oxygen vacancy or other) in most of the material studied. The mechanism of such impurity ion-defect aggregation is not clear and is worth further investigation.

REFERENCES

- [1] M. Nikl, "WIDE BAND GAP SCINTILLATION MATERIALS. Progress in the technology and material understanding," *Phys. Stat. Sol. (a)*, vol. 178, pp. 595–620, 2000.
- [2] C. W. E. v. Eijk, "Inorganic-scintillator development," *Nucl. Instrum. Methods Phys. Res. A*, vol. A460, pp. 1–14, 2001.
- [3] K. W. Kramer, P. Dorenbos, H. U. Gudel, and C. W. E. v. Eijk, "Development and characterization of highly efficient new cerium doped rare earth halide scintillator materials," *J. Mater. Chem.*, vol. 16, pp. 2773–2780, 2006.
- [4] M. Nikl, "Scintillation detectors for x-rays," *Meas. Sci. Technol.*, vol. 17, pp. R37–R54, 2006.
- [5] R. Atrata, P. Schauer, J. Kvapil, and J. Kvapil, "A single crystal of YAG—New fast scintillator in SEM," *J. Phys. E, Sci. Instrum.*, vol. 11, pp. 707–708, 1978.
- [6] M. Moszynski, T. Ludziewski, D. Wolski, W. Klamra, and L. O. Norlin, "Properties of the YAG:Ce scintillator," *Nucl. Instrum. Methods Phys. Res. A*, vol. A345, pp. 461–467, 1994.
- [7] A. Lempicki, M. H. Randles, D. Wisniewski, M. Balcerzyk, C. Brecher, and A. J. Wojtowicz, "LuAlO₃:Ce and other aluminate scintillators," *IEEE Trans. Nucl. Sci.*, vol. 42, no. 4, pp. 280–284, Aug. 1995.
- [8] M. Nikl, E. Mihokova, J. A. Mares, A. Vedda, M. Martini, K. Nejezchleb, and K. Blazek, "Traps and timing characteristics of LuAG:Ce³⁺ scintillator," *Phys. Stat. Sol. (b)*, vol. 181, pp. R10–R12, 2000.
- [9] M. Nikl, H. Ogino, A. Krasnikov, A. Beitlerova, A. Yoshikawa, and T. Fukuda, "Photo- and radioluminescence of Pr-doped Lu₃Al₅O₁₂ single crystal," *Phys. Stat. Sol. (a)*, vol. 202, pp. R4–R6, 2005.

- [10] H. Ogino, A. Yoshikawa, M. Nikl, K. Kamada, and T. Fukuda, "Scintillation characteristics of Pr-doped $\text{Lu}_3\text{Al}_5\text{O}_{12}$ single crystals," *J. Cryst. Growth*, vol. 287, pp. 335–338, 2006.
- [11] M. Nikl, "Energy transfer in the luminescence of wide band-gap scintillators," *Phys. Stat. Sol. (a)*, vol. 202, pp. 201–206, 2005.
- [12] M. Nikl, E. Mihokova, J. Pejchal, A. Vedda, Y. Zorenko, and K. Nejezchleb, "The antisite lual defect-related trap in $\text{Lu}_3\text{Al}_5\text{O}_{12}:\text{Ce}$ single crystal," *Phys. Stat. Sol. (b)*, vol. 242, pp. R119–R121, 2005.
- [13] M. Nikl, J. Pejchal, E. Mihokova, J. A. Mares, H. Ogino, A. Yoshikawa, T. Fukuda, and A. V. D'Ambrosio, "Antisite defect-free $\text{Lu}_3(\text{Ga}_x\text{Al}_{1-x})_5\text{O}_{12}:\text{Pr}$ scintillator," *Appl. Phys. Lett.*, vol. 88, pp. 141916–141916, 2006.
- [14] M. K. Ashurov, Y. K. Voronko, V. V. Osiko, A. A. Sobol, and M. I. Timoshechkin, "Spectroscopic study of stoichiometric deviation in crystals with garnet structure," *Phys. Stat. Sol. (a)*, vol. 42, pp. 101–110, 1977.
- [15] C. R. Stanek, K. J. McClellan, M. R. Levy, and R. W. Grimes, "Extrinsic defect structure of $\text{Re}_3\text{AQl}_5\text{O}_{12}$ garnets," *Phys. Stat. Sol. (b)*, vol. 243, pp. R75–R77, 2006.
- [16] M. Nikl, V. V. Laguta, and A. Vedda, "Energy transfer and charge carrier capture processes in wide-band-gap scintillators," *Phys. Stat. Sol. (a)*, vol. 204, pp. 683–689, 2007.
- [17] H. Ogino, K. Kamada, A. Yoshikawa, J. Pejchal, J. A. Mares, M. Nikl, A. Vedda, J. Shimoyama, and K. Kishio, "Suppression of host luminescence in the Pr:LuAG scintillator," *IEEE Trans. Nucl. Sci.*, vol. 55, no. 3, Jun. 2008.
- [18] Y. N. Xu and W. Y. Ching, "Electronic structure of yttrium aluminium garnet," *Phys. Rev. B*, vol. 59, pp. 10530–10535, 1999.
- [19] M. J. Weber, "Optical spectra of Ce^{3+} and Ce^{3+} -sensitized fluorescence in YAlO_3 ," *J. Appl. Phys.*, vol. 44, pp. 3205–3208, 1973.
- [20] T. Takeda, T. Miyata, F. Muramatsu, and T. Tomiki, "Fast decay U.V. phosphor- $\text{YAlO}_3:\text{Ce}$," *J. Electrochem. Soc.*, vol. 127, pp. 438–444, 1980.
- [21] E. Atrata, P. Schauer, J. Kvapil, and J. Kvapil, "A single crystal of $\text{YAlO}_3:\text{Ce}^{3+}$ as a fast scintillator in SEM," *Scanning*, vol. 5, pp. 91–96, 1983.
- [22] V. G. Baryshevski *et al.*, *Nucl. Tracks Rad. Meas.*, vol. 22, pp. 11–14, 1993.
- [23] J. A. Mareš, M. Nikl, J. Chval, I. Dafinei, P. Lecoq, and J. Kvapil, "Fluorescence and scintillation properties of $\text{LuAlO}_3:\text{Ce}$ crystal," *Chem. Phys. Lett.*, vol. 241, pp. 311–316, 1995.
- [24] A. Mares, N. Cechova, M. Nikl, J. Kvapil, R. Kratky, and J. Pospisil, "J. Pospisil: Cerium-doped $\text{RE}^{3+}\text{AlO}_3$ perovskite scintillators: Spectroscopy and radiation induced defects," *J. Alloy. Comp.*, vol. 275–277, pp. 200–204, 1998.
- [25] A. G. Petrosyan, G. O. Shyrinyan, K. L. Ovanesyan, C. Pedrini, and C. Dujardin, "Bridgman single crystal growth of Ce-doped $(\text{Lu}_{1-x}\text{Y}_x)\text{AlO}_3$," *J. Cryst. Growth*, vol. 198–199, pp. 492–496, 1999.
- [26] V. G. Barishevski *et al.*, " $\text{YAlO}_3:\text{Ce}$ -fast-acting scintillators for detection of ionizing radiation," *Nucl. Instrum. Methods Phys. Res. B*, vol. B58, pp. 291–293, 1991.
- [27] S. I. Ziegler, J. G. Rogers, V. Selivanov, and I. Sinitzin, "Characteristics of the new $\text{YAlO}_3:\text{Ce}$ compared with BGO and GSO," *IEEE Trans. Nucl. Sci.*, vol. 40, no. 2, pp. 194–197, Apr. 1993.
- [28] J. Trummer, E. Auffray, P. Lecoq, A. G. Petrosyan, and P. Semper-Roldan, "Comparison of LuAP and LuYAP crystal properties from statistically significant batches produced with two different growth methods," *Nucl. Instrum. Methods Phys. Res. A*, vol. A551, pp. 339–351, 2005.
- [29] M. Fasoli, I. Fontana, F. Moretti, E. Mihokova, M. Nikl, A. Vedda, Y. Zorenko, and V. Gorbenko, "Shallow traps in $\text{YAlO}_3:\text{Ce}$ single crystal perovskites," *IEEE Trans. Nucl. Sci.*, vol. 55, no. 3, Jun. 2008.
- [30] E. Mihoková, M. Nikl, J. A. Mareš, A. Beitlerová, A. Vedda, K. Nejezchleb, K. Blažek, and C. D'Ambrosio, "Luminescence and scintillation properties of YAG:Ce single crystal and optical ceramics," *J. Lumin.*, vol. 126, pp. 77–80, 2007.
- [31] K. Takagi and T. Fukazawa, "Cerium-activated Gd_2SiO_5 single crystal scintillator," *Appl. Phys. Lett.*, vol. 42, pp. 43–45, 1983.
- [32] H. Suzuki, T. A. Tombrello, C. L. Melcher, and J. S. Schweizer, "UV and gamma-ray excited luminescence of cerium-doped rare-earth oxyorthosilicates," *Nucl. Instrum. Methods Phys. Res. A*, vol. A320, pp. 263–272, 1992.
- [33] L. Pídel, O. Guillot-Noël, A. Kahn-Harari, B. Viana, D. Pelenc, and D. Gourier, "EPR study of Ce^{3+} ions in lutetium silicate scintillators $\text{Lu}_2\text{Si}_2\text{O}_7$ and Lu_2SiO_5 ," *J. Phys. Chem. Solids*, vol. 67, pp. 643–650, 2006.
- [34] J. A. Mares, M. Nikl, E. Mihokova, A. Beitlerova, A. Vedda, and C. D'Ambrosio, "Scintillation response and comparison of behavior of Ce-doped garnets, perovskites and silicates," *IEEE Trans. Nucl. Sci.*, vol. 55, no. 3, Jun. 2008.
- [35] D. W. Cooke, B. L. Bennett, R. E. Muenchausen, J.-K. Lee, and M. A. Nastasi, "Intrinsic ultraviolet luminescence from Lu_2O_3 , Lu_2SiO_5 and $\text{Lu}_2\text{SiO}_5:\text{Ce}^{3+}$," *J. Lumin.*, vol. 106, pp. 125–132, 2004.
- [36] M. Nikl, J. A. Mares, N. Solovieva, J. Hybler, A. Voloshinovskii, K. Nejezchleb, and K. Blazek, "Energy transfer to the Ce^{3+} centers in $\text{Lu}_3\text{Al}_5\text{O}_{12}:\text{Ce}$ scintillator," *Phys. Stat. Sol. (a)*, vol. 201, pp. R41–R44, 2004.
- [37] P. Dorenbos, C. W. W. van Eijk, A. J. J. Bos, and C. L. Melcher, "Afterglow and thermoluminescence properties of $\text{Lu}_2\text{SiO}_5:\text{Ce}$ scintillation crystals," *J. Phys. Cond. Matter*, vol. 6, pp. 4167–4180, 1994.
- [38] R. Visser, C. L. Melcher, J. S. Schweizer, H. Suzuki, and T. A. Tombrello, "Photostimulated luminescence and thermoluminescence of LSO scintillators," *IEEE Trans. Nucl. Sci.*, vol. 41, no. 4, pp. 689–693, Aug. 1994.
- [39] A. Vedda, M. Martini, F. Meinardi, J. A. Mares, E. Mihokova, J. Chval, M. Dusek, and M. Nikl, "Tunnelling process in thermally stimulated luminescence of mixed $\text{Lu}_x\text{Y}_{1-x}\text{AlO}_3:\text{Ce}$ crystals," *Phys. Rev. B*, vol. 61, pp. 8081–8086, 2000.
- [40] A. Vedda, D. D. Martino, M. Martini, V. V. Laguta, M. Nikl, E. Mihokova, J. Rosa, K. Nejezchleb, and K. Blazek, "Thermoluminescence of Zr-codoped $\text{Lu}_3\text{Al}_5\text{O}_{12}:\text{Ce}$ crystals," *Phys. Stat. Sol. (a)*, vol. 195, pp. R1–R3, 2003.